Study Butte: A Chaotic Chondrite Breccia with Normal H-Group Chemistry

K. Fredriksson and E. Jarosewich
National Museum of Natural History, Smithsonian Institution, Washington, D.C. 20560

F. Wlotzka
Max-Planck-Institut für Chemie, Abt. Kosmochemie, D-6500 Mainz, FRG

Z. Naturforsch. **44a**, 945–962 (1989); received August 11, 1989

Dedicated to Professor Heinrich Wänke, on the occasion of his 60th birthday.

The Study Butte (SB) H-group chondrite is an accretionary, well-indurated, multicomponent breccia of exceptional complexity. It contains practically all previously described types of chondrules (in two discrete populations according to Fe/Mg and Al/Ca distributions) and fragments (including CAI's and also some which were not observed before, e.g. an "andesite"); furthermore it is gas-rich. According to currently popular definitions, it can be ascribed to petrographic type 3 based on overall texture, presence of glass in chondrules and the wide spread of pyroxene and olivine composition (PMD 30), although about 2/3 have nearly constant Fa 17 (PMD 4) in the normal H-range. In addition, Al and Ca in individual chondrules with normal H-olivines, Fa 16–20, are negatively correlated, as usual in chondrules from H 4.5 chondrites [3], but are positively correlated in other chondrules. Thus SB has the properties of both "equilibrated" and "unequilibrated" chondrites. However, in spite of the multitude and complexity of components, the bulk composition is that of normal H-chondrites. A great variety of multi-stage accretion and chondrule formation, break-ups, heating and compaction processes in a quasi closed system are clearly indicated; no clues to preceding nebular processes have been recognized. After the descriptive and analytical data a "Model", based upon bulk composition, for the formation of chondrules and chondrites is presented.

Introduction and Scope

The Study Butte (SB) chondrite, a single individual of 417 g, was found on September 30, 1983, by Mr. T. Turrentine. The locality is 2.2 km SSE of Study Butte, Texas, at 29°18′6″ N and 104°30′0″ W. The stone was recognized as a meteorite by Mr. R. Pugh as reported in a preliminary description [1]. The remaining main mass is in the Smithsonian meteorite collection, number USNM 6276. Figure 1 shows two views of the specimen.

The stone was classified as H3 on the basis of (original) metal and total iron content and large variations in olivine (Fa 1–26, PMD 50) and pyroxene compositions [1]. SB is a very complex breccia containing a great variety of chondrules and a number of different fragments not previously observed, or at least not assembled in a single stone. The fragments include Ca,Al-rich inclusions and "andesite". Fredriksson et al. [1] also suggested that it might be gas-rich, which has now been confirmed [2].

In the present study we describe the chemical and mineralogical compositions of chondrules, matrix and especially the exotic fragments and attempt to reconcile the variety of constituents with the normal chondritic bulk composition. Because the stone is gas-rich, studies of trace elements, isotope ratios and perhaps cosmic ray or fission tracks would also be worthwhile.

Reprint requests to Dr. F. Wlotzka, Max-Planck-Institut für Chemie, Abt. Kosmochemie, Postfach 3060, D-6500 Mainz.

Chemical Composition

A 10.6 g sample was analysed by the techniques of Jarosewich [4]. The results are reported in Table 1; column 1 contains the raw analysis and column 2 the recalculated analysis assuming that water is absent, Fe_2O_3 is Fe and SO_3 is FeS. Also included are averages and standard deviations for 26 analyses (all by E. J.) of H-chondrite falls, types 3, 4, 5 and 6. The somewhat higher FeO and lower FeS in SB ar proba-

0932-0784 / 89 / 1000-0945 $ 01.30/0. – Please order a reprint rather than making your own copy.

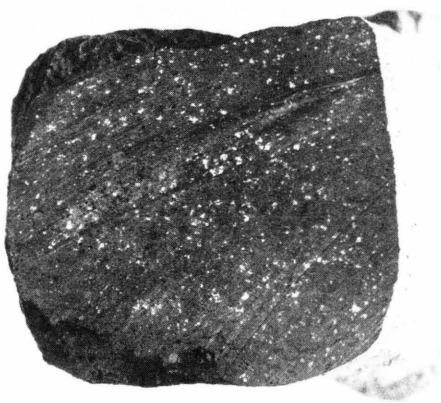

Fig. 1. Two views of the Study Butte main specimen, USNM 6276, approximately $3 \times 5 \times 6$ cm, 261 grams (top photo slightly overexposed to show the exterior). A faint brecciation and a somewhat irregular distribution of metal and sulfide are barely discernible; no extraordinary featurs for an H-chondrite are obvious.

Table 1. Wet chemical analysis (wt%) of the Study Butte Meteorite and the average of 26 H-Chondrites. Analyst: E. Jarosewich, Smithsonian Institution.

	Study Butte		H-Chondrites	
	(1)	(2)	(3)	(4)
SiO_2	34.33	37.03	36.58	0.55
TiO_2	0.13	0.14	0.12	0.01
Al_2O_3	2.06	2.22	2.14	0.15
Cr_2O_3	0.50	0.54	0.52	0.03
Fe_2O_3	14.57	–	–	–
FeO	10.93	11.79	10.31	1.18
MnO	0.28	0.30	0.31	0.02
MgO	21.39	23.07	23.26	0.39
CaO	1.81	1.95	1.74	0.09
Na_2O	0.72	0.78	0.86	0.04
K_2O	0.07	0.08	0.09	0.01
P_2O_5	0.24	0.24	0.27	0.03
H_2O^+	2.98	–	0.45	0.52
H_2O^-	0.33	–	–	–
Fe	3.75	15.04	15.96	1.56
Ni	1.38	1.49	1.73	0.09
Co	0.07	0.08	0.08	0.02
FeS	3.98	5.03	5.45	0.38
$SO_3^=$	0.63	–	–	–
C	0.20	0.22	0.06	0.04
Sum	100.35	100.00	99.97	0.38
Total Fe	24.97	26.93	27.45	0.86

(1) Original sample.
(2) Recalculated on H_2O-free basis; Fe_2O_3 reported as metal and $SO_3^=$ as FeS.
(3) Falls, grades 3 trough 6.
(4) Standard deviation.

bly due to the uncertainties involved in recalculating the raw data. The metal and troilite contents agree well with the results reported by Fredriksson et al. [1]. The total Fe, 27%, is within the H-group range and lower than the 31% given previously [1]. The latter value is probably too high due to an overestimate of FeO. The presence of small amounts of primary magnetite ($FeO \cdot Fe_2O_3$), as described below, would slightly lower the metal and FeO values. It must, however, be emphasized that the bulk composition (disregarding weathering) is close to that of normal (all?) H-chondrites in spite of the complex structures, petrology and mineralogy described in some deail below.

Petrography

Study Butte is a well-indurated, hard, accretionary breccia. It consists of a great variety of chondrules (one with olivine Fa 28, i.e. within the LL-range), more or less fragmented, and lithic fragments, sometimes equilibrated and sometimes rounded and chon-

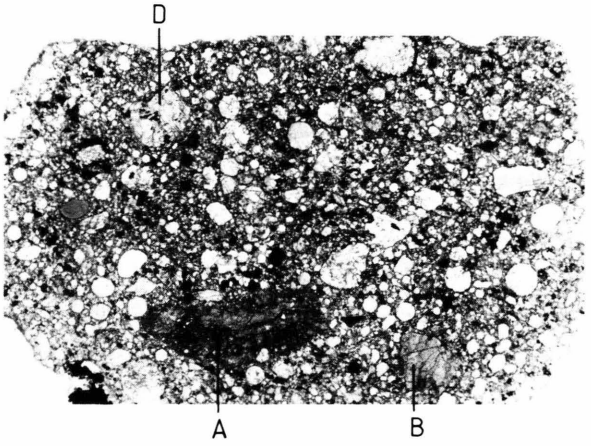

Fig. 2. Low magnification photomicrograph of SB thin section. Fragments A, B and D described in the text are indicated. Length of section, 15 mm.

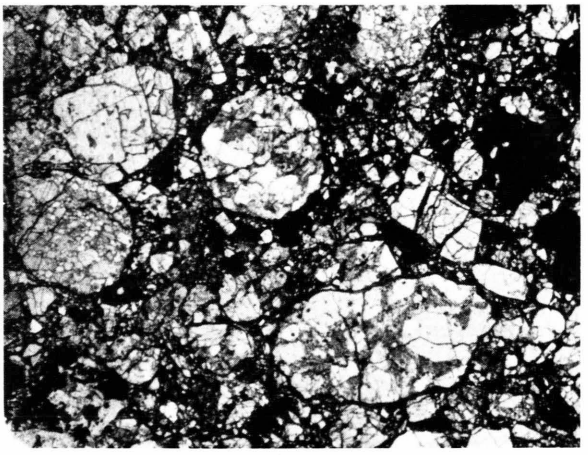

Fig. 4. Abraded lithic (or possibly chondrule) and mineral fragments, upper left, resemble chondrules. Length of section, 1.8 mm.

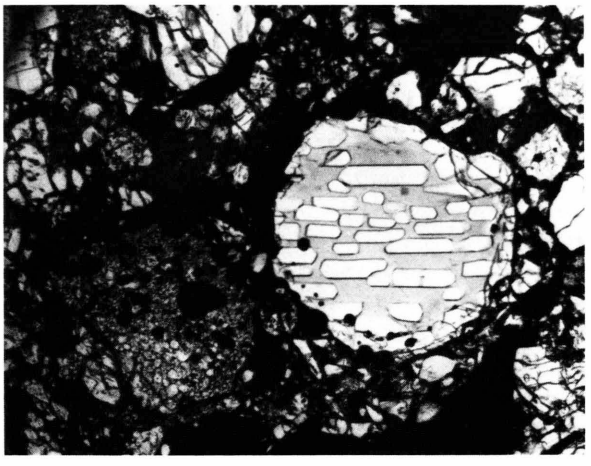

Fig. 3. A "pristine" barred, monosomatic olivine-glass chondrule; no chemical alterations appear to have occurred after its incorporation, although parts of the rim have been broken off. The olivine is Fa 0.3–2, while the glass composition is near oligoclase, but with 6% FeO. Length of section, 0.57 mm.

drule-like. Some fragments appear to be of magmatic origin. There are also discrete mineral fragments up to several hundred μm across, mainly olivine and pyroxene, but also magnetite, silica and phosphates. Metal-magnetite-cohenite aggregates and Al-rich inclusions also occur. Figure 2 is a low magnification photomicrograph illustrating this great complexity; chondrules and fragments marked are described below. Study Butte also has a vague light-dark texture which has been obscured by rather strong terrestrial weathering. This weathering is manifested by frequent Ni-bearing rims of iron oxide or brown, translucent (in thin section) hydroxides around many metal grains and as fillings in cracks, expecially in some (shocked?) fragments.

Chondrules

As most type 3 chondrites (H, L, or LL), SB contains practically all structural types of chondrules, i.e. porphyritic, barred, radiating, etc., although typical radiating pyroxene chondrules seem unusually scarce. On the other hand, some of the most perfect barred forsterite (Fa 0.3) – glass chondrules are found, Figure 3. It should be emphasized, however, that about 2/3 of the chondrules have olivine compositions between 16 and 20 mol% Fa, i.e. in the H-group range. One apparently equilibrated LL-type porphyritic, olivine-pyroxene (0.8 mm) chondrule with Fa 28–29 was also found. Other unusual, or "anomalous" chondrules contain substantial amounts of silica (probably mostly tridymite) with pyroxene. A number of rounded, chondrule-like objects could also be abraded lithic fragments as suggested in 1885 by Tschermak [5] (although erroneously for the eccentro-radial chondrules). However, rounded objects (Fig. 4), where olivine and pyroxene crystals have no apparent relation to the periphery but are abruptly cut, appear to be abraded rock fragments or abraded chondrules.

Table 2. Summary of EMP broad beam analyses (wt%) of 53 Study Butte chondrules. UEQ = chondrules with variable olivine and pyroxene composition; EQ = chondrules with constant olivine and pyroxene composition within the normal H-group range ($16 < Fa < 20$). Compare bulk silicate, Table 3 and Figs. 5 and 17. PMD = percent mean deviation.

	25 UEQ Chondrules			28 EQ Chondrules		
	Average	PMD	Range	Average	PMD	Range
SiO_2	51.5[a]	9	40 –59	49.1	5	40 –59
Al_2O_3	4.33	50	1.2– 9.9[b]	4.22	39	1.4– 8.6
CaO	2.04	46	0.7– 3.9[b]	2.45	56	0.5– 6.4
FeO	10.0[a]	28	6.5–17	14.9	24	10 –20
MgO	31.0[a]	16	22 –44	28.7	10	25 –35
Fe/Fe + Mg mol%	16	28	7 –24	22	19	18 –26
Fa (OL)[c]	7.8	78	0.3–16[d]	17.9	4	17 –19

[a] One chondrule with extreme SiO_2, 66%, and low MgO, 14%, excluded.
[b] One chondrule with extreme Al_2O_3, 0.6%, and CaO, 0.46%, excluded.
[c] 20 olivine grains, many zoned, from UEQ and 19 from EQ chondrules in thin sections.
[d] One chondrule with Fa 21, one with Fa 28, i.e. EQ LL-type, excluded.

Because SB is a well-indurated, hard rock, chondrules could not easily be separated for individual analysis. However, it has been shown [3] that in individual chondrules from type 3 ordinary chondrites (H, L, or LL), Ca, Al and Ti are positively correlated, which is not the case for types 4 and 5 where Ca and Al are anticorrelated. Thus we analyzed 54 chondrules of SB in polished thin sections by electronmicroprobe (EMP) with broad beam techniques. Uncertainties are involved due to standardization and absorption correction problems, and especially the unknown position of any one section of a chondrule relative to its real center and periphery (see Appendix).

The analyses were divided into two groups (Table 2), i.e. chondrules with variable olivine, UEQ's (unequilibrated), and those with H-group olivine, EQ's (equilibrated). Perhaps the most striking feature is that the ranges of all elements overlaps for both groups of chondrules and, at least for Al, Ca and Mg, fall within the ranges of 89 UEQ chondrules (3's) and 219 EQ chondrules (4's and 5's) from ten H, L and LL chondrites [6].

Of special interest is the Ca-Al relationship in the two groups of SB chondrules. Chondrules with olivine compositions outside the normal H-range show a positive Ca-Al correlation (Fig. 5A, UEQ). Such correlations are typical for type 3 chondrites; they were found in Tieschitz [3, 7, 8], Hallingeberg [9], Semarkona [10] and other unequilibrated chondrites [11]. However, in SB chondrules with olivine in the H-range (Fa 16–20) Al and Ca are anticorrelated (Fig. 5A, EQ). This Ca-Al anticorrelation has been found by Fredriksson in "equilibrated" H-Chondrites [3, 9], e.g. H 5 Allegan, H 4 Ochansk, L 5 Barwell and L 4 Saratov. Thus SB is partly "unequilibrated" and partly "equilibrated" also with respect to the distribution of Al and Ca. A somewhat similar situation was described by Fredriksson et al. [11] for Bjurböle (L 4). In chondrules with less than 49% SiO_2 Al and Ca are anticorrelated, as in type 4 and 5 chondrites, whereas in silica-rich chondrules Al and Ca are correlated as in the UOC's. However, in Bjurböle the two groups of chondrules have constant olivine and pyroxene compositions, unlike the two groups in SB, which differ in the olivine and pyroxene compositions, Table 2.

In Fig. 5B the CaO and Al_2O_3 contents of UEQ and EQ chondrules are plotted in a different way: chondrules are sorted in a sequence of increasing SiO_2 content. A similar plot was used in [3] and [9]. It shows again the correlation of both elements in the UEQ's and the anticorrelation in the EQ's, with the exception of the most Al-rich chondrules. In addition this plot shows the general tendency of decreasing Al with increasing SiO_2. The same tendency was observed for chondrules from Allegan, Ochansk and Tieschitz [3], as well as from Hallingeberg and Saratov [9].

It can be seen from Table 2 that in our broad beam analyses the average Al_2O_3 content of UEQ and EQ chondrules (about 4%) is substantially higher than Al_2O_3 in the bulk silicates of SB (2.6%, Table 3). This seems to be connected with the analytical method, because similar high Al_2O_3 figures were found by broad beam analysis of Tieschitz and Sharps chondrules in thin sections [7], but not by analysis of whole

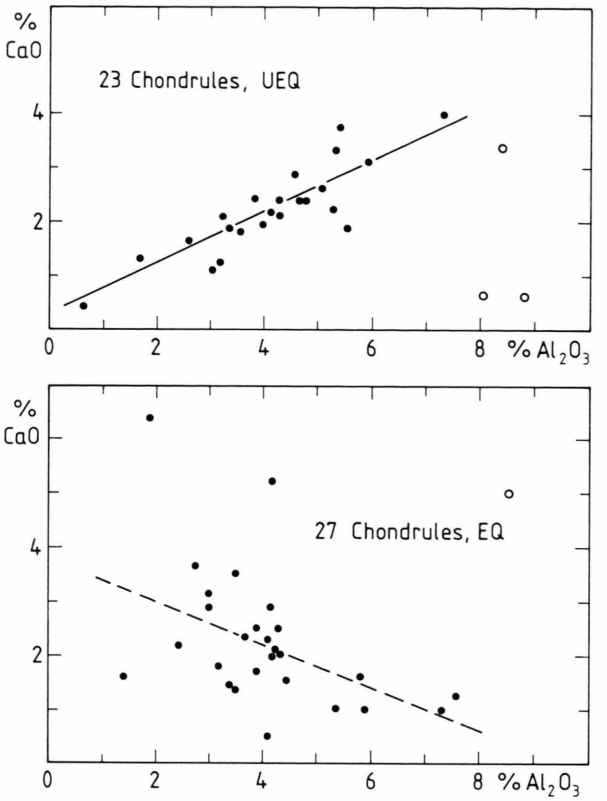

Fig. 5A. CaO vs. Al_2O_3 content (wt%) in individual SB chondrules (EMP broad beam analyses). UEQ = "unequilibrated', i.e. with varying olivine-pyroxene, mostly Fa < 16. EQ = "equilibrated", i.e. with olivine-pyroxene in the H-range, Fa 16–20. Note correlation ($r = 0.86$) of Ca and Al for UEQ's and anticorrelation ($r = -0.49$) for EQ's, r is the correlation coefficient (with exception of chondrules with more than 8% Al_2O_3, open symbols, which were not included in the correlation calculation).

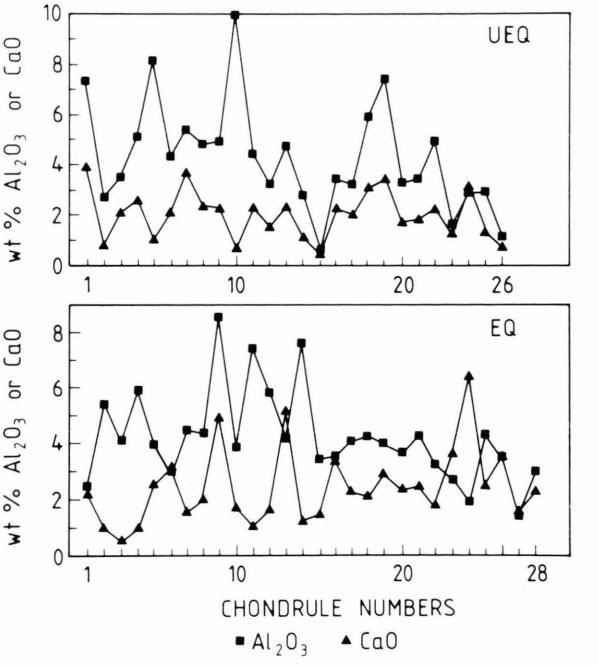

Fig. 5B. The same set of chondrules plotted in a sequence of increasing SiO_2 concentration. For both UEQ and EQ chondrules SiO_2 falls between 40 and 59%, except for one UEQ chondrule with 66% SiO_2. Note generally decreasing Al with increasing Si, compare [3, 9].

chondrules of the same or other type 3 chondrites [8–10, 12]. We therefore suspect a systematic analytical error in the broad beam analysis of thin sections, see "Appendix". This error, however, apparently does not change the Ca-Al relations shown in Fig. 5, because the same correlations and anticorrelations were observed in other chondrites by analyzing whole chondrules by the pellet method [3, 8, 9, 11].

In the following paragraphs a few chondrules having unusual textures and/or mineralogy and apparent bulk chemistry, e.g. du to an excess of silica, will be described. All common types of chondrules are present in SB. The overview photomicrograph (Fig. 2) gives some impression of textures of chondrules as well as their distribution and relation to matrix and fragments. The photomicrographs of the selected

Table 3. Study Butte fragments A, B and C (Fig. 2). EMP broad beam analyses (wt%).

	Fragment A	Fragment B	Fragment C	Bulk Silicate[a]
SiO_2	40	40	48	44
TiO_2	nd	nd	nd	0.2
Al_2O_3	2.4	2.7	3.0	2.6
Cr_2O_3	0.6	nd	nd	0.6
FeO	20[b]	14	13	14
MnO	0.1	nd	nd	0.4
MgO	25	33	29	28
CaO	1.9	1.7	2.4	2.4
Na_2O	0.4	1.4	1.1	1.0
K_2O	0.2	0.2	0.1	0.1
Ni (NiO)	1.5 (1.9)	0.3	0.3	–
FeS	8.2	4.1	1.4	6.0
Sum	101	97	98	99
Mol% Mg/Mg + Fe	69[b]	81	80	79

nd = Not determined.
[a] Recalculated from bulk analysis, Table 1.
[b] FeO is high because of oxides formed by terrestrial weathering and filling minute fractures.

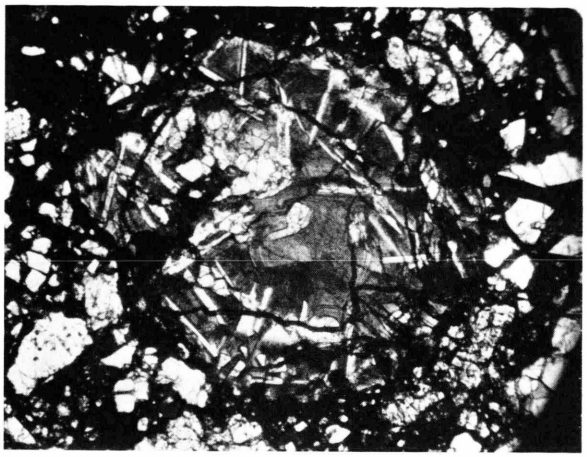

Fig. 6. Chondrule "b" consists of grey, nearly crypto-crystalline pyroxene, Fs 28, and SiO_2, probably tridymite, white, as laths and aggregates, e.g. upper left in the chondrule. Length of section, 0.57 mm.

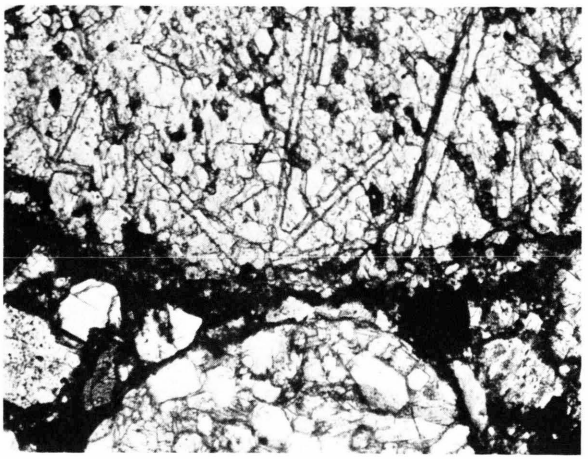

Fig. 7. Detail of chondrule "c" (upper part); it consists of enstatite, Fs 2–3, with needles of SiO_2, probably tridymite. The lower object is a partly broken porphyritic olivine-pyroxene chondrule. Length of section, 0.57 mm.

chondrules "a" through "d", Figures 3 and 6 to 8, also show some of the more common types.

Chondrule "a", shown in Fig. 3, is a classical, barred olivine/glass chondrule with exceptionally clear glass and welldefined, unfractured olivines, Fa 0.3. The glass has nearly oligoclase composition (10% Na_2O, 1.8% K_2O, 17% Al_2O_3) buth with 3% MgO and 6% FeO; its composition is rather uniform throughout the whole chondrule section. High resolution SEM of the olivine indicates a narrow (about 2 μm), rather sharply defined, more iron-rich rim (Fa 2.3) around the homogenous core. Two small opaque spherules are metal; the larger spherules are not exposed at the surface of the section. Chondrule "a" seems to be a "pristine" droplet incorporated into the matrix without disturbance or significant reactions. However, the parent material must also have had an exceptional composition because the CaO/Al_2O_3 ratio is an extreme 0.07 (wt).

Chondrule "b", Fig. 6, consists mainly of cryptocrystalline pyroxene, Fs 28, which contains laths and coarser grains of silica. The silica phase is probably tridymite, judging from the birefringence. The relation of the SiO_2 laths to the periphery indicates that "b" is indeed a chondrule, not an abraded fragment.

Chondrule "c", located near "b", also contains tridymite and is nearly spherical (Fig. 7), the diameter is 1.5 mm. It consists mostly of granular enstatite, Fs 2–3%, with needles of SiO_2, probably tridymite.

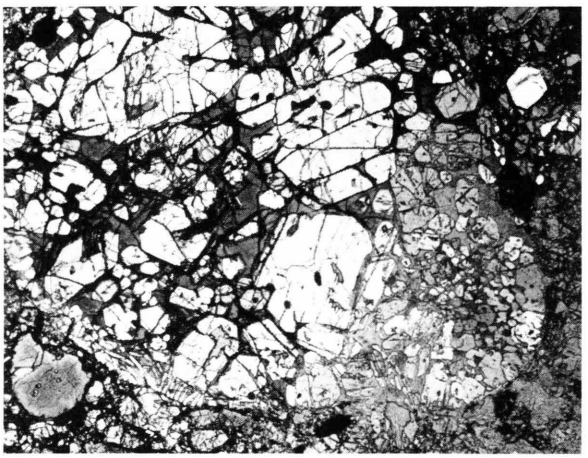

Fig. 8. Chondrule "d" appears to have an attached or invading smaller chondrule, right; more likely it originated as an extruded melt from the main part. Olivine composition is uniform, Fa 17.5. Length of section, 1.7 mm.

Again, the relation to the periphery evinces its origin as a "droplet" chondrule. The different pyroxene compositions show that there was no "communication" between the droplets "b" and "c" before or after accretion and indicate differences in parent materials and cooling and crystallization histories.

Chondrule "d", Fig. 8, is a multiple chondrule. It consists of a larger, coarser round part with olivine, Fa 17.5, and mesostasis from which a smaller half

spherule, right, seems to protrude. This smaller part has the same olivine composition but apparently less mesostasis. The texture does not indicate a collision between two particles. Rather, it seems likely that when the large drop cooled and began to crystallize, some liquid was extruded and crystallized relatively faster. This behavior has been observed experimentally by Fredriksson [13] and also seems to explain the origin of the *monosomatic* olivine-glass "double" chondrule described by Tschermak [5], Figure 74.

Fragments

The range of lithic, chondrule and mineral fragments and inclusions with regard to size, chemistry, mineralogy, morphology, etc., found in SB is bewildering. It is nearly impossible to describe all types in detail; rather, we have attempted to study broad classes into which most (observed to date) seem to fit. The uncertainty in distinguishing some rounded, abraded rock (or chondrule) fragments from true chondrules further complicates matters, as does the presence of "splinters" of individual minerals (described below, "Mineralogy"). However exotic some types of fragments appear, none seems to influence the bulk composition. In the following paragraphs the common rock fragments are described, but no serious attempt has been made to determine the relative abundance, although generally types A, B and C are more common (and larger) than the following, while type G is unique in our sections.

Fragment A, Fig. 2, is a typical shocked rock fragment, 1.5 × 5 mm, which may well have been a breccia before its incorporation into SB, with which it is well integrated. A few anhedral olivine crystals have normal H-chondrite composition (Fa 18–19). A small, rounded part near the center appears to have had a shock vein before incorporation into fragment A. The approximate bulk composition obtained by electron-probe analyses (broad beam) is given in Table 3. The FeS content is higher than in the bulk, but there is practically no metal. However, terrestrial "oxides" are present. Thus the total Fe content, 21%, is about 7% lower than in the bulk, while the Mg/Mg+Fe mol ratio is only 0.69 compared to 0.78 for the bulk. Yet, fragment A is essentially a black, i.e. shocked [14], H-chondrite without metal.

Fragments B (Fig. 2, Table 3) and C (Table 3) are also finegrained and probably of similar origin as A. However, FeS and total Fe decrease from A to B to C, which is reflected in increased transparency of the thin sections. The Mg/Mg+Fe mol ratios for B and C are 0.81 and 0.80, respectively, close to the 0.78 for the bulk analysis.

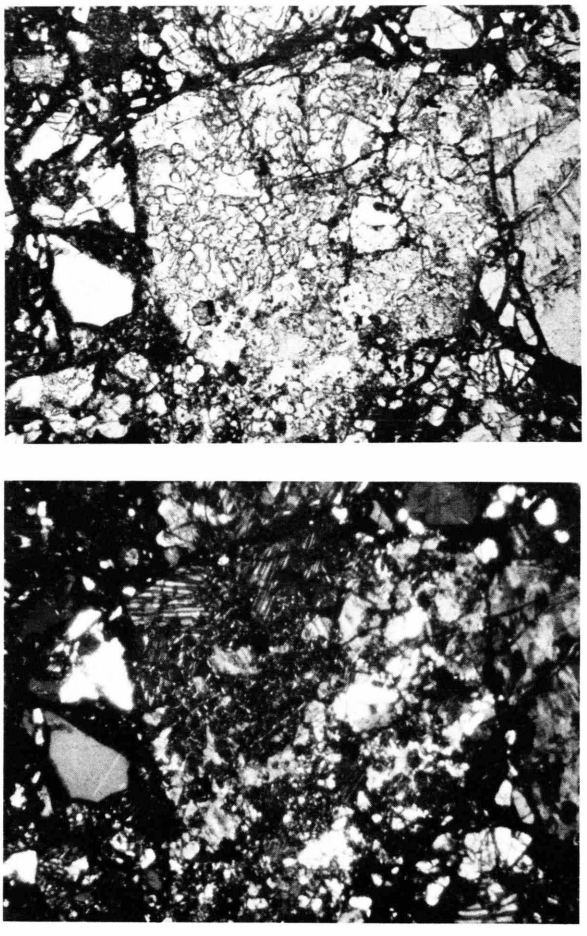
(a)

(b)

Fig. 9. Photomicrographs in ordinary light (a) and polarized light (b). Fragment "E" consists of different pyroxenes, silica, and one olivine, Fa 20. The silica is mostly in the left part of the fragment, dark in "b", with small white lines (cracks), while the olivine grain is white. Twinned pyroxene is at upper left. Length of section, 0.57 mm.

Fragment D, 1.5 mm across (Fig. 2), is from an H-chondrite and has a type 6 texture. It contains coarse, fractured olivine and pyroxene grains within the H-range, plus metal and troilite. The small amount of mesostasis has nearly oligoclase composition with about 4% Cr_2O_3. Twinned plagioclase crystals (an important criterion for type 6) are present.

Fragment E, Fig. 9, consists of pyroxenes with varying compositions, silica and one olivine grain, Fa 20.

Fig. 10. Photomicrographs in ordinary (a) and polarized light (b). Andesitic fragment "G" (see text) consists of diopsidic pyroxene and twinned plagioclase, An 40–50. Note the broken-off fragments, left, with matrix invading the cracks, indicating a not too gentle accretion. Bulk and phase composition are given in Table 4. Length of section, 0.2 mm.

This assemblage is hard to explain unless fragment E itself is from a mechanical breccia which was never heated after its own or the SB accretion.

Fragment F (90 × 230 μm) consists largely of SiO_2 (probably tridymite) and orthopyroxene, Fs 32, one of the most iron-rich found. A few small laths of augite, Wo50 En15 Fs35, are also present. One of the SiO_2-bearing chondrules ("b") described above also has iron-rich pyroxene, while another ("c") contains almost pure enstatite, Fs 3. This type of fragment, but differing in the proportions of the minerals, is not uncommon.

Fragment G, Fig. 10a, b, was considered unique until one of us (FW) serendipitously found a cluster of four almost identical fragments in a small area of a thin section of Beddgelert (H4, our classification). All five fragments have an andesitic bulk composition, Table 4, and consist of slightly zoned diopsidic pyroxenes, Wo40 En53 Fs7, and zoned plagioclase in the range An40–50 with traces of Fe and Mg but only about 0.2% K_2O, i.e., more calcic than normal chondritic feldspar (An15). Interstitial glassy mesostasis is present, its composition is given in Table 4. These andesitic fragments have igneous textures distinctly different from the textures of chondrules or chondritic lithic fragments. The plagioclase forms a network of primary euhedral crystal laths, in which the pyroxene (here diopside) is interstitial. In normal chondrules or lithic fragments this is reversed; plagioclase is xenomorphic and interstitial to pyroxene. The Beddgelert andesites also contain some relatively large grains of olivine and orthopyroxene which, remarkably, have the same H-type composition, i.e. Fa 17.9 and Fs 15.7, as in the rest of the meteorite. These andesites appear to have been derived by differentiation on a parent body, but it is noteworthy that the bulk composition is close to the average ("differentiated") compositions of the mesostases reported in Table 6, except for higher MgO and CaO and lower alkalies in the andesites, Table 4. The occurrence of these clasts in two different H-chondrites indicates that lava-type melt rocks may not be uncommon on the H-chondrite parent body. Another igneous, differentiated rock-type was found by Hutchison et al. [15] in the Barwell chondrite. The clustering of the Beddgelert fragments and the fracturing of the SB fragment (Fig. 10) are probably due to late brecciation during a complex accretion.

Fragment H is a 100 × 200 μm fine-grained dark aggregate similar in composition to scarce matrix lumps and rims (Table 5), it will be discussed with them under "Matrix" below.

Ca, Al-Rich Inclusions

Ca- and Al-contents in bulk chondrules vary and may reach 7% CaO and 10% Al_2O_3, usually the result of a high amount of Al-rich mesostasis (see below) in an otherwise normal chondrule. For instance, chondrule "a", the barred olivine chondrule described above, contains 8.8% Al_2O_3 (broad beam analysis), which corresponds to about 50% mesostasis. How-

Table 4. Composition of andesite clasts. EMP analyses.

	Study Butte, Fragment G				Beddgelert, Clast 1		
	Bulk*	Plagioclase	Glass*	Diopside	Bulk*	Plagioclase	Diopside
SiO_2	59	57.3	62	54.6	57	58.1	51.7
Al_2O_3	18	27.1	13	2.93	17	27.5	3.44
FeO	2.6	0.21	1.6	3.27	3.2	0.21	4.0
MgO	5.7	0.15	6.1	17.9	9.5	0.29	17.2
CaO	9.3	9.23	8.5	19.2	8.8	8.77	20.1
K_2O	0.4	0.15	1.3	–	0.3	0.28	–
Na_2O	5.2	6.01	5.9	0.70	5.3	6.1	0.79
TiO_2	nd	nd	1.4	1.42	0.5	0.1	1.23
Sum	100	100.2	100	100.0	102	101.4	98.5
		An 45 Or 1 Ab 54		Wo 42 En 53 Fs 5		An 44 Or 2 Ab 55	Wo 43 En 51 Fs 6

nd = Not determined. * Broad beam analyses.

Table 5. Composition of fine-grained matrix, lumps and rims, see Figs. 15, 16. EMP broad beam analyses.

	Lumps			Rims					Average (8)	SB Bulk[a]
	Frag H	M2	M3-1	M1	M3-2	M4	M5	M7		
SiO_2	31.1	33.5	31.5	31.1	31.1	33.4	37.0	32.0	32.6	35.9
Al_2O_3	3.1	6.3	2.1	3.3	1.9	3.3	2.0	3.5	3.2	2.2
FeO	37.4	39.4	44.5	44.4	41.6	43.7	35.5	40.7	40.9	33.6
MgO	25.2	13.7	16.9	16.0	21.8	16.6	23.0	19.3	19.1	22.4
CaO	0.8	3.4	0.9	1.4	0.6	0.8	0.8	1.2	1.2	1.9
NiO	2.5	2.9	3.9	3.0	2.5	1.8	1.4	2.7	2.6	2.3
S	0.2	0.3	0.3	0.4	0.3	0.3	0.3	0.6	0.3	1.8
Sum[b]	100	100	100	100	100	10	100	100	100	100

[a] All Fe as FeO. [b] Normalized to 100%.

ever, there are also other Ca, Al-rich bodies, so-called CAI's. They are in the size range 50 to 200 μm and usually show a concentric texture, where rounded, very fine-grained areas are surrounded by a clear rim (Figure 11). The rims consist of diopside or, in one case, of Al, Ti augite (fassaite), similar to those described in H3 Tieschitz by Wlotzka [7]. The interior material is a fine-grained intergrowth of spinel and a silicate mesostasis which has a Na- and Al-rich feldspathic composition, sometimes tending towards sodalite (5% Cl, 13% Na_2O, 37% Al_2O_3). In the particle shown in Fig. 12, however, this mesostasis consists of melilite (Åk 4 to 15), which also surrounds the spinel area in a clear mantle 10 to 20 μm wide. Besides spinel, small grains of perovskite (up to 5 μm across) are also present. The whole assemblage is covered on two sides by a layered rim containing first very fine spinel and perovskite (less than one μm grains), followed by an outer diopside layer of about 5 μm.

Magnetite-Metal-Cohenite Inclusions

Magnetite occurs in single, sometimes euhedral grains and in complex inclusions. It is then intergrown with sulfide and metal, sometimes also with cohenite and graphite. In one such inclusion (Fig. 13), cohenite (2% Ni), kamacite (6–7% Ni), graphite and magnetite (no detectable Ni) form 30 to 100 μm grains, whereas taenite (54–58% Ni) occurs as a 5 μm rim between magnetite and kamacite, or as small grains. Sulfide is present as 10 to 20 μm grains in the magnetite. The texture of the inclusion is somewhat obscured by secondary, terrestrial iron oxide, but it seems clear that magnetite forms the outer and metal the inner part of it. Magnetite shows mostly a straight, sometimes euhedral external surface. Cohenite occurs on one side of the inclusion and graphite on the other in rather large grains not intergrown with other phases. The inclusion also has small (about 10 μm) grains of the most

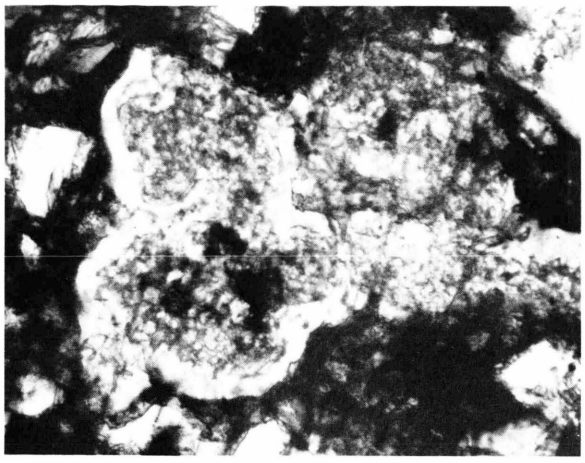

Fig. 11. CAI consisting of a core of fine-grained, Na, Al-rich feldspathic material and spinel with a rim of diopside, apparently twinned. Length of section, 0.125 mm.

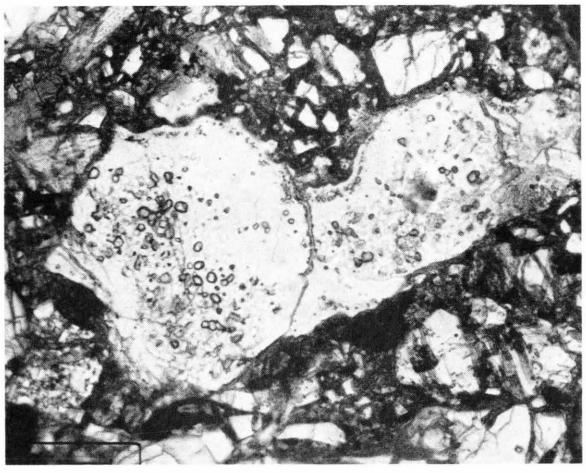

Fig. 12. CAI consisting of a melilite mantle (Ak 4 to 15) with spinel and small perovskites (high relief grains) in the middle, surrounded by a narrow layered rim (see text); the outermost part, about 5 μm, is diopside. Note also the coarse matrix consisting of clastic debris. Length of section, 0.18 mm.

iron-rich olivine, Fa 29, and pyroxene, Fs 35, found. Other magnetite inclusions are more rounded and have the size of chondrules (some hundred μm). Usually they contain small grains (tens of μm) of metal and/or sulfide, and sometimes a metal core. In the inclusion shown in Fig. 14 the core consists of both kamacite and taenite.

Similar inclusions have been reported only from "the most unequilibrated" LL-chondrites [16, 17]. In

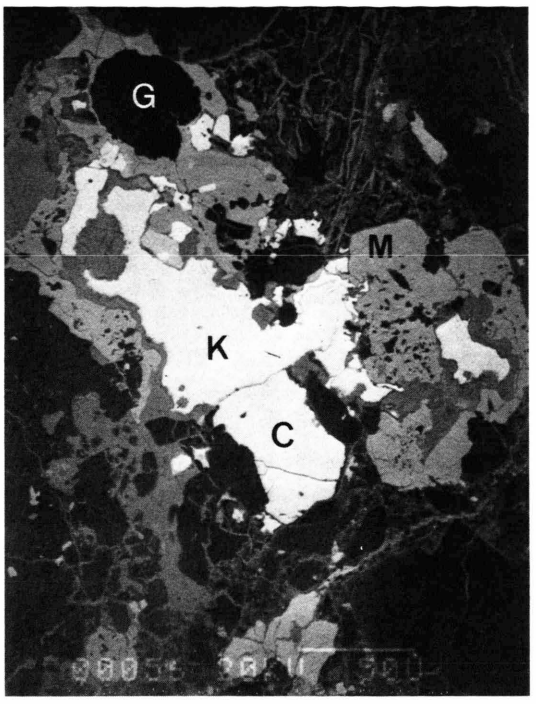

Fig. 13. Inclusion consisting mainly of kamacite (K), cohenite (C), magnetite (M) and graphite (G). Dark grey material, mainly between metal and magnetite, is terrestrial ironoxide. Silicates are black. SEM picture, scale bar 50 μm.

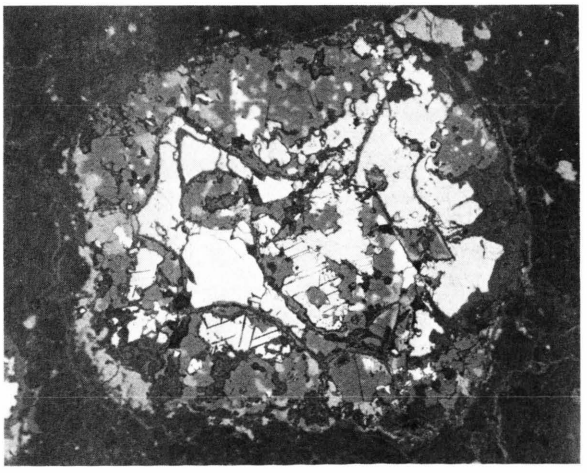

Fig. 14. Subrounded magnetite-metal inclusion, etched, reflected light. Magnetite (dark grey) surrounds a metal core (white) consisting of kamacite (showing Neumann bands in places) and taenite. Small grains of troilite (lighter grey) in the magnetite. Darker grey veins and patches are terrestrial iron oxides. Length of section, 0.6 mm.

SB it seems that they formed by oxidation of metal to magnetite, because the magnetite surroundes a metal core which looks corroded (Figure 14). In an intermediate stage carbide and graphite were formed. This indicates drastic changes in the environment (carbon, oxygen) of these metal grains. However, this happened before agglomeration of the SB meteorite and affected only a few of the metal grains, others having remained unchanged. Hutchison et al. [17], who found spherical carbide/metal/sulfide objects in the UOC Semarkona, concluded from their morphology that some carbide and magnetite crystallization occurred after accretion.

Matrix

The matrix filling the interstices between chondrules and fragments in SB comprises rather coarse, clastic debris of the normal chodritic silicates (see Figure 12). The fine-grained opaque or translucent matrix normally found in type 3 chondrites [18, 19] is absent as a groundmass. It is found, however, in rare "matrix lumps" and coating a few chondrule fragments.

The matrix lumps, except for the relatively large fragment H (Fig. 15), are 20 to 50 μm across and consist of a fine-grained (below 10 μm), translucent aggregate of iron-rich olivines (Fa ≈ 25) with narrow, more iron-rich rims (up to Fa 43). Sometimes they include irregular iron sulfide grains (5 to 20 μm), which may contain up to 15% Ni. A few large chondrule fragments are discontinously coated by the same type of translucent matrix; it is especially thick over surface indentations (up to 50 μm), Figure 16. It is noteworthy that this matrix covers irregular, fractured surfaces; it was not observed on primary, smooth chondrule surfaces or embayments in them. This differs from observations by Scott on other unequilibrated chondrites [20].

The composition of matrix lumps and rims was determined by broad beam microprobe analysis (avoiding the iron-rich weathering products), see Table 5. The elements Na, K, Ti, Cr and Mn were detected in minor amounts (< 1%) and not quantitatively determined. All compositions are similar to each other and to bulk SB, except that bulk SB has more S and lower total Fe (expressed as FeO). Also the Ca/Al ratio of the matrix (average 0.51) is lower than in bulk SB, 1.17. Similar trends were observed for other type 3 chondrite matrices [7, 18, 21]. The enrichment of FeO is noteworthy and may be explained by the addition of a fayalite component; the compositions plot more or less along a line connecting forsterite and fayalite (Figure 17). The same trend was found in the matrix of the LL3 chondrite Krymka [21]. The average total Fe/Ni ratio of 15.3 is not far from the C1 ratio of 16.9 [22]. However, C in the matrix areas is

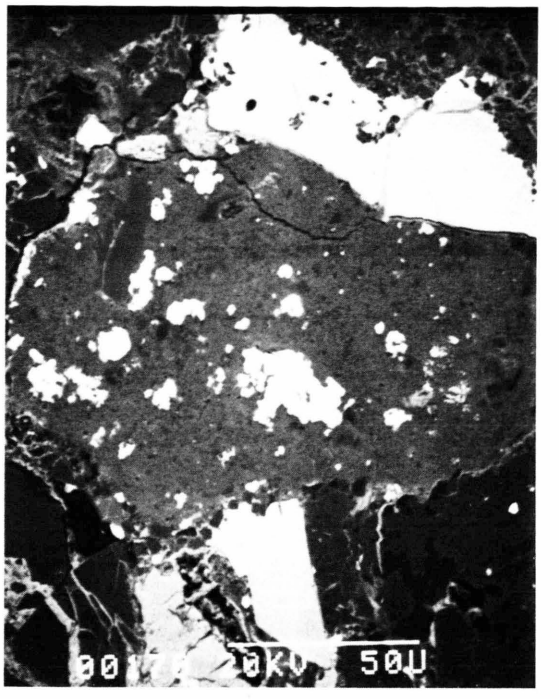

Fig. 15. Matrix "lump", scanning electron microscope image. It consists of finegrained iron-rich olivine, the white grains are iron sulfides. Scale bar 50 μm.

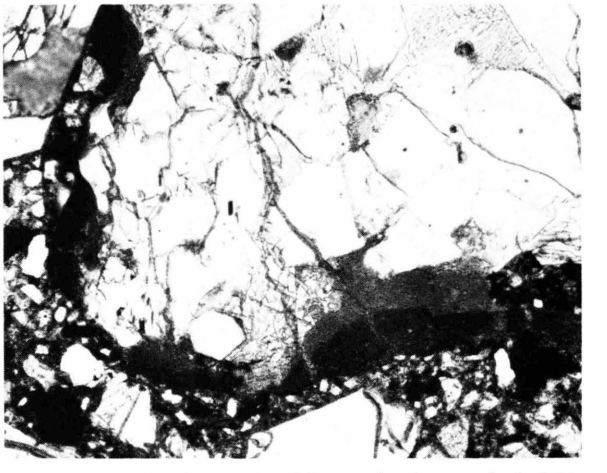

Fig. 16. Irregular fragment with matrix rim, analysis M1, Table 5. Note differences in transparency with no significant change in composition. Length of section, 0.18 mm.

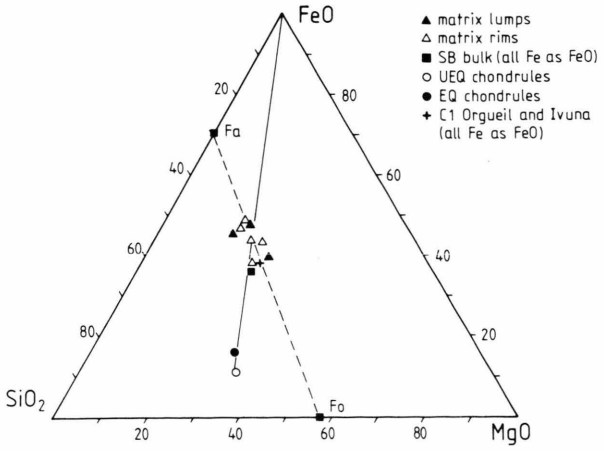

Fig. 17. SiO_2, MgO and FeO (wt%) plot for matrix lumps and rims, compared with the chondrule population and C1 Orgueil and Ivuna. Fa = fayalite, Fo = forsterite.

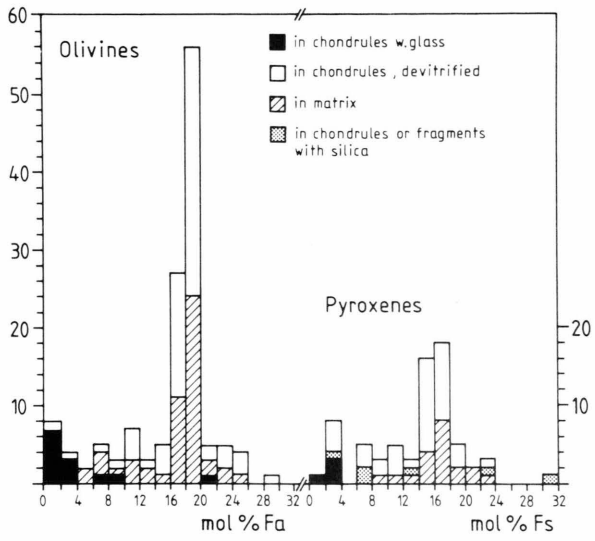

Fig. 18. Distribution of iron content in olivines (Fa) and in pyroxenes (Fs). Overall average for Fa (135 grains) is 16.1 (%MD = 30), for Fs (70 grains) 13.6 (%MD = 32).

below the detection limit of 0.5% C. The SB chondrules (UEQ's and EQ's), on the other hand, are approximately collinear with the FeO-apex (Fig. 17), the "matrix" cluster and SB bulk silicates; a genetic relation is indicated.

Mineralogy

Olivine occurs in chondrules, fragments and matrix with varying composition as indicated by the histogram in Figure 18. The Fa and Fs distributions are bimodal (compare Table 2); with maxima at low iron content and in the normal H-group range; note also the similarity in matrix and chondrules, indicating that the matrix largely formed from broken chondrules. This is consistent with the observation that almost all matrix olivines are fragments or splinters, e.g. Figs. 3 and 12. Again, about 2/3 of the olivines are in the H-range, 16–20 mol% Fa, while the total range is Fa 0.3 to 29 with PMD of 30. Euhedral crystals are common in some chondrules but scarce in lithic fragments and matrix, at least in the size range we have observed; euhedra may be present in the ultrafine matrix, "holy smoke" [23].

Zoning in individual grains is not common or strong, although most forsteritic olivines (Fa <1) in glassy chondrules seem to have a narrow, sharp rim with slightly more iron. Some porphyritic chondrules do have zoned olivines; the extreme range observed is Fa 11 (center) to Fa 17 (rim), the latter within the H-range.

Pyroxenes

Ca-poor pyroxene occurs in both orthorhombic and monoclinic forms. The composition is as variable as that of the olivines, ranging from Fs 1 to 24, with Fs 28 in a SiO_2-bearing chondrule (Figure 6) and Fs 32 in a rock fragment also containing silica. The distribution shows a distinct peak at the normal H-chondrite values, Fs 14–18 (Fig. 18), but, as for olivines, it is also bimodal and similar in devitrified chondrules and matrix. It is also significant that pyroxenes in SiO_2-bearing chondrules and fragments span the whole range. Moderate zoning was observed in several grains. The Fs values are usually lower than the Fa values of coexisting olivine. Exceptions are found in chondrules with clear mesostasis glass and low Fs values (range in four chondrules: Fs 1 to 4, average 2.1); in two such chondrules Fs is slightly higher than Fa in coexisting olivines. Diopside occurs in some "equilibrated" chondrules as narrow rims on Ca-poor pyroxene, especially in the LL-type chondrule described above and in the andesite fragment.

Figure 18 shows that olivines and pyroxenes in chondrules with clear glass have very low FeO contents (compare chondrule "a" described above). The same trend was observed in the H3 chondrites Tieschitz and Sharps [7]. Chondrules with clear glass are only found in unequilibrated chondrites and consid-

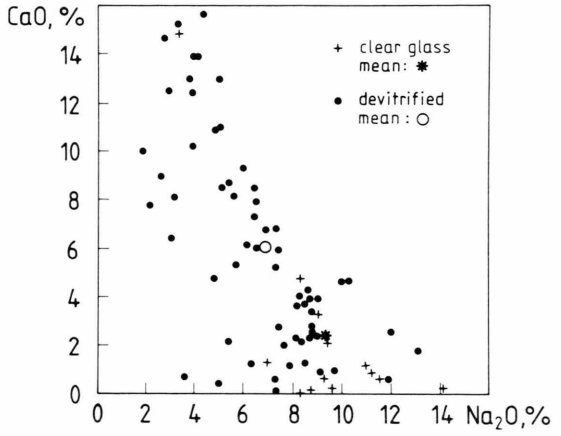

Fig. 19. CaO vs. Na_2O in the mesostasis of individual chondrules. Glasses are in general on the Na-rich side of the distribution.

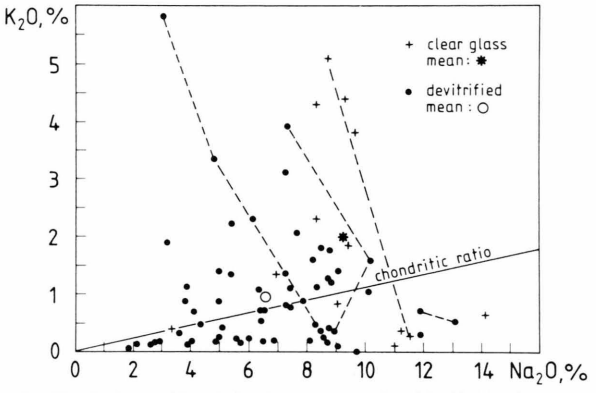

Fig. 20. K_2O vs. Na_2O in the mesostasis of individual chondrules. Analyses within the same chondrule are connected with dashed lines.

Table 6. Average composition of chondrule mesostases. EMP analyses. (In brackets: number of chondrules analyzed).

	Mesostases			
	Glass (13)		Devitrified (62)	
	Wt%	Std. Dev.	Wt%	Std. Dev.
SiO_2	58.8	3.8	61.8	5.7
TiO_2	0.45		0.40	
Al_2O_3	20.7	3.4	17.2	6.0
Cr_2O_3	0.43		0.35	
FeO	2.65	1.4	2.60	2.4
MgO	3.02	3.4	3.70	3.3
CaO	2.29	4.0	6.00	4.4
K_2O	2.0	1.8	1.0	1.0
Na_2O	9.3	2.5	6.6	2.5
Sum	99.6		99.5	

ered to be primitive. Their low FeO content may thus be connected with the chondrule forming process, i.e. point to reducing conditions.

Glass and Mesostasis

The mesostasis of chondrules may be a clear, isotropic glass, but mostly it is cryptocrystalline or consists of a fine intergrowth of feldspar and diopsidic pyroxene. The composition was measured by broad beam electronprobe techniques and found to be generally Si, Al and alkali-rich, but varies from chondrule to chondrule. Figures 19 and 20 give the the CaO–Na_2O and K_2O–Na_2O relations. Glasses tend to be on the Na-rich and Ca-poor side of the distribution. This is also seen in the average composition of the glasses compared to the "devitrified" (i.e. cryptocrystalline or crystalline) mesostases, see Table 6. The large K-Na variations shown in Fig. 20 are noteworthy. Different K and Na contents were sometimes measured in different areas of the same chondrule (connected points in Fig. 20), thus the Na_2O/K_2O ratios in Fig. 20 are not necessarily valid for whole chondrules. Still, also bulk chondrules show a large range in Na/K ratios, compare [10]. Large variations in Na and K content were also found in chondrule mesostases of the H3 chondrites Tieschitz and Sharps [7].

Phosphates

Both chlorapatite and whitlockite occur as 100 to 200 μm single crystal fragments in the matrix, but are sometimes intergrown with olivine.

Opaque Phases

The usual opaque minerals of equilibrated chondrites, i.e. metal, troilite and chromite, are found in SB, in addition magnetite and Cr-spinel; cohenite and graphite occur in special inclusions, which were described above.

Metal is coarse-grained (typically 50 to 500 μm) and usually equidimensional, only grains in chondritic lithic fragments show more irregular outlines. Both kamacite and taenite occur, occasionally also tetrataenite [1]. Kamacite shows abundant Neumann bands when etched, often mechanically deformed.

Troilite is finer-grained than metal (typically 20 to 100 μm); most grains are single crystals and are not associated with metal.

Magnetite occurs associated with metal, cohenite and troilite in the inclusions described before, but also in isolated grains in the meteorite matrix (grainsize 20 to 100 μm). They are distinguished from the secondary iron oxides by their clean, partly euhedral appearance, which suggests that they are primary. Their content of minor elements, e.g. Ni, Mn, Cr, is $<0.1\%$.

Spinel is variable composition, it ranges from chromite to pure Mg-spinel as in other type 3 chondrites [24]. It is found in the mesostasis of chondrules and fragments (grainsize tens of μm), in the meteorite matrix (same grainsize) and in much smaller grains in Al-rich inclusions.

Discussion

From the 400 g Study Butte specimen we have studied less than 5% (20 g). How much of the parent body our sample represents, is, of course, unknown, but it seems safe so assume that it is an almost infinitesimally small fraction, in fact so small that no "terrestrial" geologist would accept it as representative for any rock unit, sedimentary or magmatic/metamorphic. The chondrite sample, however, seems to perfectly represent, chemically, all so-called H (high iron) chondrites, and that in spite of the extreme complexity which we have demonstrated.

To recapitulate: there are at least two populations of chondrules, one with constant olivine and pyroxene compositions typical of types 4 to 6 H-chondrites, the other with variable, sometimes zoned, olivines and pyroxenes as in type 3's and mostly with lower iron content, Table 2. The two populations are also clearly distinguished by their Al_2O_3/CaO relations, Figure 5. In addition, exotic fragments range from silica to magnetite-graphite-metal. The bulk composition of Study Butte still remains within the close range for H-chondrites, Table 1, while only about 2/3 of the olivines and pyroxenes are in the Grade 4 to 6 ("equilibrated") range for H-chondrites.

We believe that there are two major problems which are not satisfactorily explained by currently popular nebular condensation models for chondrule formation followed by accretion and/or "metamorphism" in some unknown environment. The problems so well illustrated by SB are the same for the two other chondrite iron groups, L (low iron) and LL (low iron, low metal), because there is no plausible reason to assume different chondrule formation or accretion processes for these groups.

1. Why is the bulk composition within each chemical group nearly constant in spite of grossly varying structures (types 3 to 6) and chondrule and mineral compositions? Apart from total iron content and its redox-state the difference between H, L and LL is also small, chemically and structurally.

2. Why do the high iron (H) chondrites have low iron silicates, and the low iron (L and LL) chondrites have the high iron silicates with little metal? This problem is obviously related to redox conditions, but again, how and why?

The problems become especially vexing if, justifiably, the processes for chondrule/chondrite formation are assumed to be similar, or rather the same, on each of the three (or more) distinct H, L and LL parent bodies.

Thus we feel motivated to present a crude "model" based on our SB data and known processes, and to be critical of the more nebulous chondrule formation processes [25–27]. Our model accords with the growing consensus that chondrules formed from preexisting "aggregates" on planetary bodies [28, 29]. We envision formation from a "soil", i.e. material homogeneous on more than cm, inhomogeneous on less than mm scales. This concept has now convincing terrestrial analogues, e.g. the micro-irghizites [30] and the "chondrite" formations in South Africa [31, 32].

Any hypothesis for the origin of chondrules and chondrites must first take into consideration the following primary features: 1) Bulk chemistry, 2) Mineralogy, i.e. phase relations, and 3) Structural and textural properties. Subordinate features, e.g. isotopic anomalies and trace element fractionations, cannot be used as the criteria to construct singular models, if they contradict the primary features.

A "Model"

The following calculations and speculations are primarily intended to emphasize the nearly constant bulk composition within the iron groups of chondrites. For this we use the hard data presented in Table 7. We do not intend to explain all features and "anomalies" in chondrites, especially not the origin of individual SB fragments, although we believe they are best produced

Table 7. Analysis of C1 Ivuna (in atoms), and of chondrites of different groups, normalized to the 58 Si atoms of Ivuna. The columns I-C2, I-H etc. give the difference between Ivuna and this chondrite, i.e. the number of atoms removed. For the enstatite chondrite E6 the analysis was also normalized to Mg in Ivuna (I-E, Mg). Fe-Met indicates the number of Fe atoms still in the chondrite as metal, not removed.

	C1 Ivuna [34]	C2 Murray [34]		H5 Allegan [35]	L6 Leedey [36]	LL6 Karatu [4]	E6 Pillistfer [35]	
	I	C2	I-C2	I-H	I-L	I-LL	I-E, Si	I-E, Mg
Si	58	58	–	–	–	–	–	+10
Mg	61	59	2	7	7	7	15	–
Fe	52	46	6	4	18	24	9	1
Fe-Met	–	+	–	(31)	(13)	(2)	(38)	(44)
Ni	3	2	1	0	1	2	0	0
Ca	5	4	1	2	2	2	3	2
C	62	28	34	61	61	61	61	61
S	32	11	21	26	26	28	20	18
O	408	318	90	214	212	202	238	207
H	318	168	150	316	318	314	318	318
	1000	694	−305	−630	−645	−640	−664	−607 (+10 Si)

on a parent body (-ies). Nor do we intend to extrapolate back beyond the accretion of these "primitive aggregates".

Thus, in the beginning, that is before the first chondrules formed, there existed, *for our purpose*, dark, cold bodies, consisting of rather unconsolidated nebular condensates, aggregates similar in composition to C1-silicates (i.e. with secondary materials like sulfates excluded), but probably with a much higher abundance of gases. The H, L and LL progenitors may have been established already at this stage either together on several bodies or as individual bodies. Our observations give no clues to this question, but it is also not of importance for the following discussion. However, based on our Study Butte results and on calculations by Fredriksson [33], we attempt to show that from *purely chemical considerations* any ordinary chondrite could be formed directly from such C1-like parents (but not L from H or LL or vice versa). Because all SB components together make a perfect H-chondrite, we propose that they had a common parent material close to the SB matrix lumps and the C1-chondrites Ivuna and Orgueil (see Fig. 17) which subsequently was altered and fragmented in a closed system.

To demonstrate, we have calculated Wiik's analysis of C1 Ivuna [34] to 1000 atoms (I in Table 7) and then normalized analyses of a C2, an H5, an L6, an LL6 and an E6 chondrite [34–36, 4] to the 58 Si atoms obtained for Ivuna, as shown in Table 7, column C2, for Murray. Column I-C2 thus is the difference between Ivuna and Murray and shows how many atoms have to be removed to obtain the Murray composition from Ivuna. Similarly the Columns I-H etc. show the number of atoms removed to obtain the H, L, LL, or E chondrite compositions. The removal of 7 atoms Mg for the H, L and LL presents a problem, as it would require fractionation of Mg from Si (the E chondrites present a different problem, see below). However, a new analysis of Orgueil by E. J. [in 37], almost identical to Ivuna [34], shows that some 6 of the 7 excess Mg atoms are present in watersoluble phases and thus do not represent the "primitive silicates". This could eliminate the long standing argument about the differences in Mg/Si ratios between ordinary and C-chondrites.

The only processes necessary are

1) Chondrule formation at high temperatures and reducing conditions which produce metallic nickel-iron, plus discriminate loss of some metal as liquid, and
2) Agglomeration of chondrules, metal and matrices in various stages of transformation.

There is enough carbon to reduce all iron oxides in Ivuna. To form H-chondrites much of the iron is reduced, but not removed, i.e. 31 atoms remain as metal, only 4 of the original 52 are removed, Table 7 column I and I-H, respectively. In contrast, for the LL-group less iron is reduced; 24 atoms remain as oxide, but

most of the metal is removed (forming the iron meteorites?) and only 2 atoms of metallic iron remain. The L-group falls between these extremes. Conceivably the redox conditions would be controlled by C–CO–CO_2 and Fe–FeO equilibria such that certain stages corresponding to the equilibrated H, L and LL olivine/pyroxene compositions would form preferentially.

Impacts indubitably were a (the?) major geological process in the early Solar System. Thus multiple impact events on and between parent bodies of various sizes are favoured as the major chondrule/chondrite forming process (as already discussed by Urey [38]). Condensation models require perfect mixing of components that formed under vastly different conditions, as in SB, and thus seem inconceivable. Impacts, possibly between or on primitive, gas-rich bodies of low density, but also on partially or totally molten bodies [39, 40] combined with impact triggered "volcanism" would provide: 1) Local heating and melting, 2) Very high and variable temperatures and cooling rates, and 3) Gas clouds (plasma) with extremely high temperatures and densities, cooling rapidly and resulting in non-equilibrium condensation. Continued impacts on once established H, L or LL chondritic bodies or regions on a body would not significantly change Mg/Fe ratios, but would destroy more chondrules, than produce new ones, the result being stronger compaction, i.e. higher petrographic types.

Impact formation of chondrules has been discussed by other authors [41, 42]. Grossman writes in his recent review and discussion about chondrule formation [42]: "Impact on planetary bodies ar first appears to be an excellent mechanism for generating chondrules. The process certainly happened, and provides enough energy to melt target material. Such melting events would involve rapid heating. Cooling could be sufficiently fast, but could be prevented from reaching extremely high rates by imbedding chondrules in an opaque cloud or an ejecta blanket. The target material may be heterogeneous and would be at the appropriate (low) temperature." The main argument against this process [41, 42] is that it seems to be too ineffective, as the impact transformed lunar and achondrite parent body regoliths contain only few chondrules. This may be different, however, if he starting material is not a regolith of solid mineral particles, but an aggregate of porous, volatile-rich condensates. Thus our "Model" is in fact a combination of Grossman's "Nebular Models" (with nebular dust as precursor material of chondrules) and "Planetary Settings or Mechanisms" (with impact melting as the formation mechanism). Bodies of such nebular dust aggregates were probably present only in the early period of Solar Sytem history. This would remove also the other argument against impact formation of chondrules [41, 42]: Their uniformly old ages of 4.4–4.5 Gy, whereas impacts on planetary bodies like the moon continued at least up to 3.9 Gy ago. Other "regolith processes" known from chondrites, like the solar wind implantation [43], can have taken place after chondrule formation in a regolith already consisting of chondrules and fragmented particles.

Finally it is suggested that E-chondrites (see Table 7, column E-I) may be more representative of rapid, direct condensates from impact clouds than the ordinary chondrites. Such clouds would be enriched in Si and heavy volatiles over Mg. Heavy volatiles are less abundant than in C-chondrites, but much higher than in ordinary chondrites (except in the ultrafine matrix [23]). Upon complete, fast condensation of such clouds the excess Si and heavy volatiles would be preserved.

Appendix

Broad Beam Electronprobe Analysis: Defense and Caution

Electronprobe analysis using a wide beam, 50 to 100 μm in diameter, or by scanning an area of equivalent size in order to obtain "bulk" analyses of small amounts of material in polished sections has become increasingly common. The technique is frequently used with believable results e.g. on pellets of finegrained material [3], or on melt beads (even when partly crystallized) or in finegrained matrix in sections of e.g. meteorites. The errors made by applying the normal absorption and fluorescence corrections to these heterogeneous samples have already been discussed [44].

We want to address a different problem here: broad beam analysis when used on sections containing rather coarse components, especially, if the components are not homogeneous in three dimensions. A typical example is analysis of chondrules (as in this work) where the location of a section with regard to the center of an often inhomogeneous object is not known. A case in point are our SB analyses, Table 2 and Fig. 5, versus the results for Tieschitz with broad beam on thin sections by Wlotzka [7] and on pellets of

isolated chondrules by Fredriksson [3]. For Al and Na the SB results by broad beam agree with those for Tieschitz, in that the average for the chondrules is higher than for the bulk. However, the pellet analysis (also by microprobe) for Tieschitz and another H3 chondrite, Dhajala, gave a lower Al (and Ca) average for chondrules than in the bulk [8]. The pellet technique has been checked against analysed chondrite silicates (also used as standards). Analyses of isolated Richardton (H5) chondrules by Evensen et al. [45] also agreed well especially with regard to the Ca, Al ratios.

Thus we presently suspect that the broad beam analyses give high estimates for Al and Na, and to a lesser degree for Ca, because of geometric effects, i.e. a random section may in some cases favor the chondrule mesostasis containing all the Al and Na. However, we felt justified to use the results for SB, especially our Table 2 and Fig. 5 (with the caveat that Al and Ca? may be too high), because of the consistency of the different Al–Ca relations in UEQ and EQ chondrules, respectively, which were also obtained by the pellet technique for other H3 vs. H4, 5 chondrites [3, 8, 9, 11].

Finally it should perhaps be emphasized that even if statistical counting and correction errors can be eliminated [44], the problem with threedimensional inhomogeneities cannot. This is shown by the following experiment: 12 randomly selected Bjurböle chondrules (L4), about 1 mm in diameter, were first cut at about 1/3 of the radius, then in a 2nd cut through the center. There were three groups with four chondrules in each, i.e. with poor (A) medium (B) and good (C) fit of the analyses for the two cuts. The following Table shows the results for one chondrule from each of these groups:

		SiO_2	Al_2O_3	CaO	MgO	FeO
Chondrule A	1st cut	53.1	4.3	3.4	22.4	13.1
	2nd cut	48.1	2.8	1.1	28.8	17.3
Chondrule B	1st cut	42.4	4.9	1.9	29.6	18.8
	2nd cut	44.1	5.9	2.4	27.5	17.4
Chondrule C	1st cut	43.8	4.5	2.4	28.3	17.8
	2nd cut	44.6	4.5	2.3	27.4	17.4

Acknowledgment

We are grateful to B. J. Fredriksson for computer evaluation and diagrams of the analytical data. Mr. J. Nelen greatly facilitated the electronprobe analyses. Our two reviewers, R. Hutchison and G. Kurat, helped us to correct and clarify a number of details and also induced us to elucidate the purpose of the "Model" (but not to change it). The Smithsonian Research Opportunities Fund, Fellowships and Grants, and the Max-Planck-Institut für Chemie, Mainz, provided funds for travel expenses which is gratefully acknowledged.

[1] K. Fredriksson, R. S. Clarke, and R. Pugh, Meteoritics **19,** 225 (1984).
[2] H. Weber, Personal Communication (1987).
[3] K. Fredriksson, Crystallinity, Recrystallization, Equilibration, and Metamorphism in Chondrites, in: Chondrules and Their Origins (E. A. King, ed.). Lunar Planetary Institute Houston (1983).
[4] E. Jarosewich, Geochim. Cosmochim. Acta **30,** 1261 (1966).
[5] G. Tschermak, Die mikroskopische Beschaffenheit der Meteoriten, E. Schweizerbart, Stuttgart 1885.
[6] K. Fredriksson amd B. Fredriksson, Meteoritics **22,** 380 (1987).
[7] F. Wlotzka, Composition of Chondrules, Fragments and Matrix in the UOC's Tieschitz and Sharps, in: Chondrules and Their Origins (E. A. King, ed.). Lunar Planetary Institute Houston (1983).
[8] K. Fredriksson, Lunar Planet. Sci. **XIX,** 352 (1988).
[9] K. Fredriksson, Lunar Planet. Sci. **XIII,** 233 (1982).
[10] J. N. Grossman and J. T. Wasson, The Composition of Chondrules in Unequilibrated Chondrites, in: Chondrules, and Their Origins (E. A. King, ed.). Lunar Planetary Institute Houston (1983).
[11] K. Fredriksson, S. V. S. Murty, and K. Marti, Meteoritics **20,** 347 (1985).
[12] J. L. Gooding, K. Keil, T. Fukuoka, and R. A. Schmitt, Earth Planet. Sci. Letters **50,** 171 (1980).
[13] K. Fredriksson, Meteoritics **21,** 364 (1986).
[14] K. Fredriksson, P. S. De Carli, and A. Aramae, in: Space Res. III (W. Priester, ed.). Proc. 3d Internat. Space. Sci. Symp., North Holland, Publ. Co. (1963).
[15] R. Hutchison, C. T. Williams, V. K. Din, R. N. Clayton, C. Kirschbaum, R. L. Paul, and M.E. Lipschutz, Earth Planet. Sci. Letters **90,** 105 (1988).
[16] G. J. Taylor, A. Okada, E. R. D. Scott, A. E. Rubin, G. R. Huss, and K. Keil, Lunar Planet. Sci. **12,** 1076 (1981).
[17] R. Hutchison, C. M. O. Alexander, and D. J. Barber, Geochim. Cosmochim. Acta **51,** 1875 (1987).
[18] G. R. Huss, K. Keil, and G. J. Taylor, Geochim. Cosmochim. Acta **45,** 33 (1981).
[19] E. R. D. Scott, A. E. Rubin, G. J. Taylor, and K. Keil, Geochim. Cosmochim. Acta **48,** 1741 (1984).
[20] E. R. D. Scott, Smithson. Contr. Earth Sci. **26,** 73 (1984).
[21] F. Wlotzka, Meteoritics **18,** 423 (1983).
[22] H. Palme, H. E. Suess, and H. D. Zeh, Landolt-Börnstein New Series, Vol. VI/2a, 257. Springer, Berlin 1981.
[23] E. R. Rambaldi, K. Fredriksson, and B. J. Fredriksson, Earth Planet. Sci. Lett. **56,** 107 (1981).
[24] F. Wlotzka, Meteoritics **22,** 529 (1987).

[25] J. A. Wood, Earth Planet. Sci. Lett. **70,** 11 (1984).
[26] G. R. Huss, Earth, Moon, and Planets **40,** 165 (1988).
[27] G. Kurat, Phil. Trans. Roy. Soc. Lond. **A 325,** 459 (1988).
[28] J. L. Gooding, K. Keil, T. Fukuoka, and R. A. Schmitt, Earth Planet. Sci. Lett. **50,** 171 (1980).
[29] R. Hutchison, C. M. O. Alexander, and D. J. Barber, Phil. Trans. Roy. Soc. London **A 325,** 445 (1988).
[30] B. P. Glass, K. Fredriksson, and P. V. Florensky, J. Geophys. Res. **88,** Suppl. B319 (1983).
[31] D. R. Lowe and G. R. Byerly, Lunar Planet. Sci. **XIX,** 693 (1988).
[32] D. R. Lowe and G. R. Byerly, Geology **14,** 83 (1986).
[33] K. Fredriksson, Meteoritics **4,** 172 (1969).
[34] H. B. Wiik, Geochim. Cosmochim. Acta **9,** 279 (1956).
[35] E. Jarosewich and B. Mason, Geochim. Cosmochim. Acta **33,** 411 (1969).
[36] E. Jarosewich, Geochim. Cosmochim. Acta **31,** 1103 (1967).
[37] K. Fredriksson and J. F. Kerridge, Meteoritics **23,** 35 (1988).
[38] H. C. Urey, J. Geophys. Res. **64,** 1721 (1959).
[39] H. Wänke, Lunar Planet. Sci. **XII,** 1139 (1981).
[40] H. A. Zook, Lunar Planet. Sci. **XII,** 1242 (1981).
[41] G. J. Taylor, E. R. D. Scott, and K. Keil, Cosmic Setting for Chondrule Formation, in: Chondrules and Their Origins (E. A. King, ed.). Lunar Planetary Institute Houston (1983).
[42] J. N. Grossman, Formation of Chondrules, in: Meteorites and the Early Solar System (J. F. Kerridge and M. S. Matthews, eds.). The University of Arizona Press, Tucson 1988.
[43] H. E. Suess, H. Wänke, and F. Wlotzka, Geochim. Cosmochim. Acta **28,** 595 (1964).
[44] H. Y. McSween, Geochim. Cosmochim. Acta **41,** 1843 (1977).
[45] N. H. Evensen, S. R. Carter, P. J. Hamilton, R. K. O'Nions, and W. I. Ridley, Earth Planet. Sci. Lett. **42,** 223 (1979).